Proceedings of the 6th International Conference on Mechanics and Materials in Design,
Editors: J.F. Silva Gomes & S.A. Meguid, P.Delgada/Azores, 26-30 July 2015

PAPER REF: 5710

BENDING RESISTANCE OF PARTIALLY ENCASED BEAMS AT ELEVATED TEMPERATURE: ADVANCED CALCULATION MODEL

Paulo A. G. Piloto[1(*)], David Almeida[2], A. B Ramos-Gavilán[3], Luís Mesquita[2]

[1]LAETA - INEGI / UMNMEE, Polytechnic Institute of Bragança, Bragança, Portugal
[2]Polytechnic Institute of Bragança, Bragança, Portugal
[3]Department of Mechanical Engineering (EPSZ), University of Salamanca, Spain
[(*)]*Email:* ppiloto@ipb.pt

ABSTRACT

Partially Encased Beams (PEBs) are composite steel and concrete elements in which the web of the steel section is encased by reinforced concrete. The experimental investigation of the bending resistance was already verified in fire and under elevated temperature (Paulo A. G. Piloto *el al*., 2013a) (Paulo A. G. Piloto *el al*., 2013b). The three-dimensional finite element solution, with precise detail of each component (steel profile, reinforcement, stirrups and concrete) was used to determine the bending resistance under three point bending configuration. Four temperature levels were tested (20, 200, 400 and 600 ºC) and three lengths were considered (2.5, 4.0 and 5.5 m), using three different cross section types, based on the dimensions of IPE100, IPE200 and IPE300 steel profiles. Two distinct types of welded stirrups were simulated (PEBA with "C" shape stirrups welded to the web and PEBB with "I" shape stirrups welded to the flange). The solution method is incremental and iterative (arc length), based on geometric and material non-linear analysis (ANSYS), using reduced integration method. Results are in accordance to the new formula presented (P. M. M Vila Real *et al.*, 2004) and adapted to partially encased beams. The bending resistance was not significantly influenced by the type of welded stirrup.

Keywords: Partially Encased Beams, Numerical simulation, Fire, Elevated temperature, Composite Steel and Concrete.

INTRODUCTION AND STATE OF THE ART

Partially Encased Beams (PEB) are composite steel and concrete elements that present several advantages with respect to bare steel beams. They are usually built with hot rolled sections with encased concrete between flanges. There are different design solutions, considering the variable of longitudinal reinforcement of concrete, the stirrup shape configuration and the material strength. The reinforced concrete between flanges increases fire resistance, corrosion resistance, load bearing, bending stiffness, without enlarging the overall size of bare steel cross section. Fire design, according to Eurocode EN1994-1-2 (CEN, 2005a), is valid for composite beams, based on tabulated methods (considering simple supporting conditions and standard fire exposure) based on prescriptive geometry to achieve specific fire rating (time domain). The simple calculation method may also be applied to PEB, assuming no mechanical resistance of the reinforced concrete slab (considering simple supporting conditions and standard heating fire from three sides). The effect of fire on the material characteristics is taken into account, either by reducing the dimensions of the parts or by reducing the characteristic mechanical properties of materials.

Partially Encased Beams (PEB) and Columns (PEC) have been widely tested at room temperature, but only a small number of experiments under fire and elevated temperature conditions have been reported. In 1987, J. B. Schleich (Schleich et al., 1987) was the project leader of an important experimental and numerical campaign developed to test and analyze the behavior of PEC and PEB with and without connection to the slab. This project demonstrated the possibilities of the computer code CEFICOSS, able to cover most structural fire applications. Karl Kordina (K. Kordina, 1989) presented tables to be used in fire design guides, based on experiments. These results were prepared to several construction elements, including PEC and PEB, for certain degree of utilization, supporting conditions and materials. Kindmean et al. (Kindmean et al., 1993) performed thirteen tests on PEB with and without concrete slabs, showing the importance of the reinforced concrete between flanges in determining the ultimate bending moment. Hosser et al. (Hosser et al., 1994), carried out four experimental tests on simply supported composite PEB, connected to reinforced concrete slabs, under fire conditions. Temperature changes were registered at different locations, including the PEB cross section. Authors concluded that the effective width of the slab depends on the transversal longitudinal shear reinforcement. Lindner and Budassis (Lindner et al, 2000), tested lateral instability at room temperature using twenty two full-scale PEB with two different steel sections under three-point bending test. A new design proposal for lateral torsional buckling was proposed, taking into consideration the torsional stiffness of concrete. R. Maquoi et al. (R. Maquoi et. al, 2002), improved and implemented knowledge on lateral torsional buckling of beams, including PEB, and prepared design rules that were not satisfactorily covered by the existing standards. Assi et al. (Assi et al., 2002), developed a theoretical and experimental study on the ultimate moment capacity of PEB, performing twelve bending tests on specimens with four different IPE cross sections, to investigate the contribution of different types of concrete. Nakamura et al. (Nakamura et al., 2003), tested three partially encased girders with longitudinal rebars and transversal rebars (welded (W) and not welded (NW) to flanges). The bending strength of the partially encased girder was almost two times higher than conventional bare steel girders. Authors concluded that the specimen with rebar not welded (NW) to flanges presented a decrease of 15 % for maximum load bearing when compared to the welded rebar (W) specimen. More recently, Akio Kodaira et al. (Akio Kodaira et al., 2004), decided to determine fire resistance of eight PEB, with and without concrete slabs. Authors demonstrated that reinforcement is effective during fire. In 2008, Elghazouli and Treadway (Elghazouli et al., 2008), performed ten full scale tests on PEB. The experimental analysis was focused on inelastic performance, considering major and minor-axis bending tests. Authors discussed several parameters related with the capacity and ductility with relevance to design and assessment procedures. De Nardin and El Debs (De Nardin et al.,2009), studied the static behaviour of three composite PEB under flexural loading at room temperature, testing some alternative positions for shear studs, using one type of mono-symmetric steel section. Experimental results confirmed that studs are responsible for the composite action and increase bending resistance, especially when the studs are vertically welded on the bottom flange. A. Correia and João P. Rodrigues (A. Correia et al., 2011), studied the effect of load level and thermal elongation restraint on PEC, built with two different cross sections, under fire conditions. They concluded that the surrounding stiffness had a major influence on fire element behaviour for lower load levels. The increasing of the surrounding stiffness was responsible for reducing critical time. Critical time remained practically unchanged for higher load levels. In 2012, Kvočák and Drab (Kvočák et al., 2012), decided to test the bending resistance of partially encased beams with slender web (class 4), using different shear stirrups and web stiffeners and concluded that the stability of slender web increased with the concrete. Recently, Paulo Piloto et al (Paulo Piloto et al., 2013a),

tested fifteen PEB under fire conditions (small series) using three-point bending test to determine fire resistance. Results revealed the dependence of fire resistance on load level. Particular emphasis was given to the critical temperature on the composite section. Paulo Piloto et al. (Paulo Piloto et al., 2013b) determined the PEB bending resistance at elevated temperature (20, 200, 400 and 600 ºC) and compared also the resistance and the post buckling deformation behaviour with bare steel beams.

PARTIALLY ENCASED ELEMENTS

A total of 72 PEB models were simulated, showing conservative results with respect to the simple calculation method. The bending resistance of PEB was determined by numerical simulation and determined for different load events (The proportional limit force F_p; the force F_y using the intersection method between two straight lines drawn from linear and non-linear interaction of the vertical displacement; the load event for the displacement limits $F_{L/20}$ and $F_{L/30}$; and the maximum load level for the asymptotic behaviour of lateral displacement F_u). The lateral torsional buckling analysis is presented for three types of cross section, two types of stirrups shape, three different lengths and four temperature levels. Table 1 presents the main characteristics of each beam under simulation also with mesh information (number of elements and nodes). Three-point bending test was considered, see Fig. 1. Special boundary conditions to simulate fork supports were defined. Each simulation used an incremental and iterative procedure to determine the bending resistance.

Table 2- Characteristics of PEB to be simulated at elevated temperature.

Id.	Reinf. [mm]	Stirrups Dim. [mm]	Stirrups shape	stirrups spacing (S) [m]	Lt [m]	Ls [m]	Nodes Number	Elements Number
PEBA100_2,4F	Ø10	Ø6	C	0,167	2,5	2,4	187473	171648
PEBA100_3,9F	Ø10	Ø6	C	0,167	4,0	3,9	290301	266112
PEBA100_5,4F	Ø10	Ø6	C	0,167	5,5	5,4	404415	370944
PEBA200_2,4F	Ø12	Ø6	C	0,100	2,5	2,4	200165	183600
PEBA200_3,9F	Ø12	Ø6	C	0,100	4,0	3,9	321195	294984
PEBA200_5,4F	Ø12	Ø6	C	0,100	5,5	5,4	439565	403920
PEBA300_2,4F	Ø20	Ø6	C	0,171	2,5	2,4	197715	182240
PEBA300_3,9F	Ø20	Ø6	C	0,171	4,0	3,9	312375	288320
PEBA300_5,4F	Ø20	Ø6	C	0,171	5,5	5,4	427035	394400
PEBB100_2,4F	Ø10	Ø6	I	0,167	2,5	2,4	187473	171648
PEBB100_3,9F	Ø10	Ø6	I	0,167	4,0	3,9	290301	266112
PEBB100_5,4F	Ø10	Ø6	I	0,167	5,5	5,4	404415	370944
PEBB200_2,4F	Ø12	Ø6	I	0,100	2,5	2,4	257985	238000
PEBB200_3,9F	Ø12	Ø6	I	0,100	4,0	3,9	321195	294984
PEBB200_5,4F	Ø12	Ø6	I	0,100	5,5	5,4	439565	403920
PEBB300_2,4F	Ø20	Ø6	I	0,171	2,5	2,4	197715	182240
PEBB300_3,9F	Ø20	Ø6	I	0,171	4,0	3,9	312375	288320
PEBB300_5,4F	Ø20	Ø6	I	0,171	5,5	5,4	427035	394400

The cross section of each PEB was defined taking into account the characteristics of the materials, the arrangement of longitudinal and transverse reinforcing steel, EN1994-1.2 (CEN, 2005a), see Fig. 2. Special arrangements were necessary to undertake, in order to accommodate composite sections with small steel profile. PEB were built with stirrups welded to the web, C-shape (PEBA), and with stirrups welded to the flange, I-shape (PEBB).

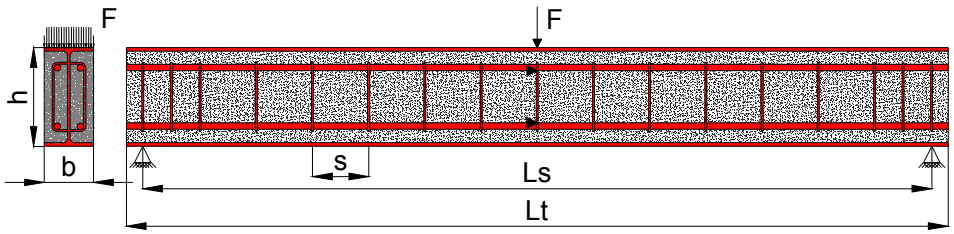

Fig. 1 - Simple supported PEB with three point bending simulation.

Fig. 2 presents all six different cross sections in analysis. Three different lengths between supports (L_S = 2.4, 3.9 and 5.4 m) were analysed. PEB were considered laterally unrestrained with exception to the supports, where two fork supports were simulated.

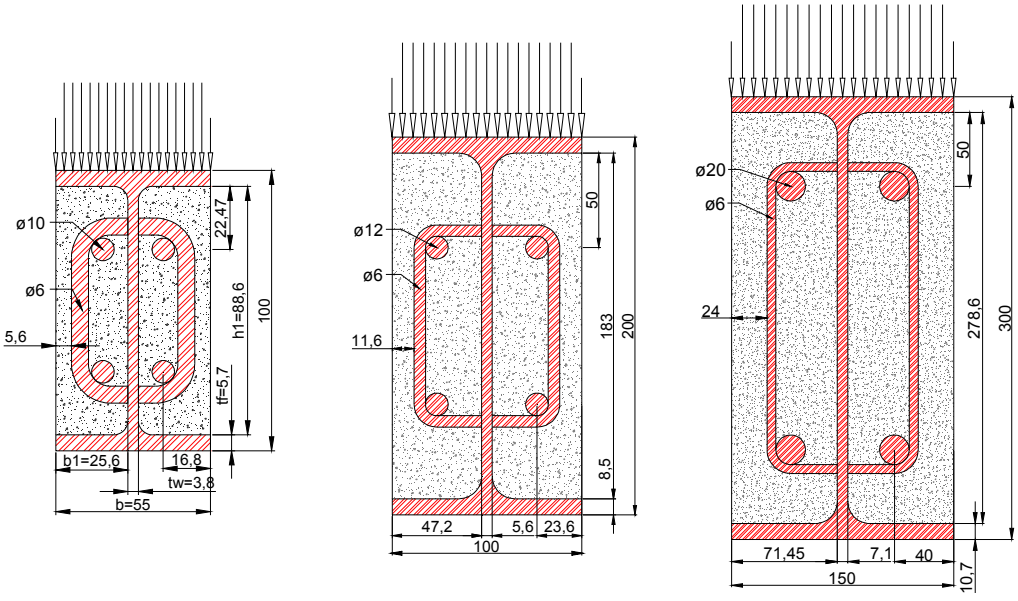

a) PEBA100 b) PEBA200 c) PEBA300

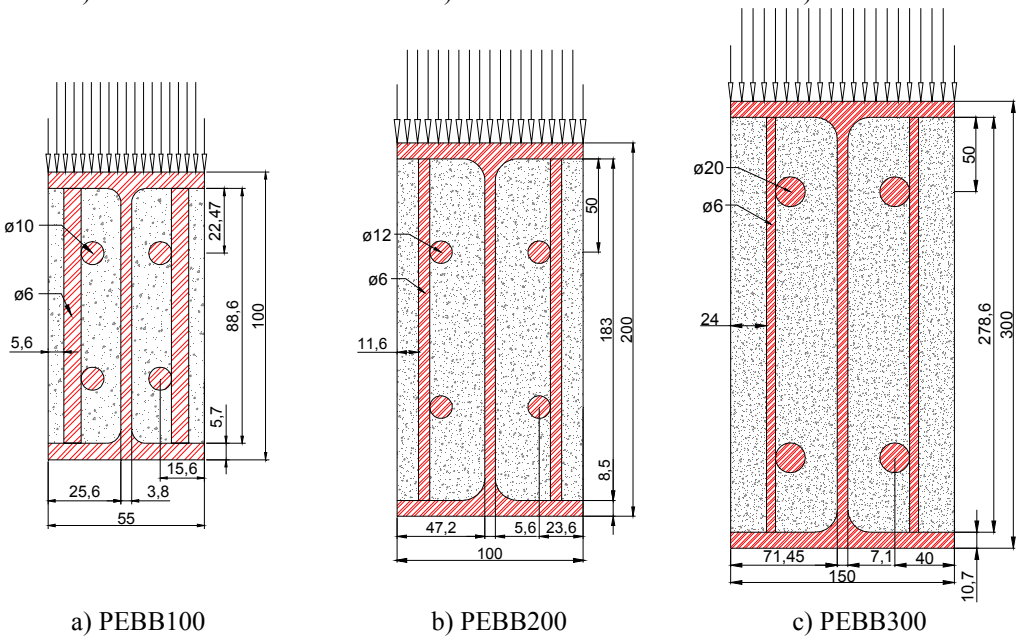

a) PEBB100 b) PEBB200 c) PEBB300

Fig.2 Six different cross section used in PEB.

BENDING RESISTANCE: SIMPLE CALCULATION METHOD

The bending resistance of the cross section may be determined by the capacity of the cross section to form a plastic hinge and by the capacity of the structural element to avoid lateral torsional buckling, see Fig. 3. To increase visibility of rebar and stirrups, one side of the encased concrete was removed from the post buckling deformed shape model.

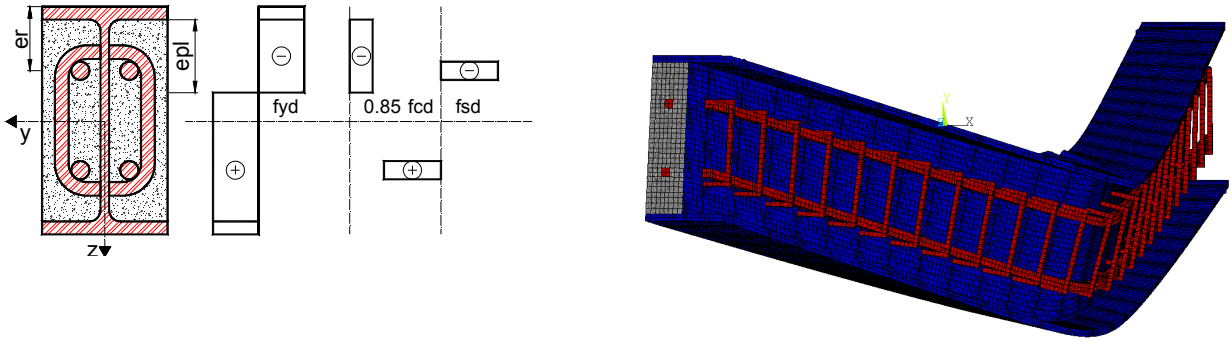

(a) Plastic Hinge (b) Lateral torsional Buckling

Fig. 3 - Ultimate Limit States for bending resistance of PEB.

The geometric properties of the composite section should consider the effect of both materials, being the concrete part taken in to account by the homogenized steel section method. Certain hypotheses were taken into to account, regarding the inertia characteristics of the cross section, in particular: the warping constant I_w of the concrete part is neglected for the benefit of an easy application, the torsion constant I_t and the second order moment of inertia I_z, are calculated by the summation of the steel part and the homogenized part of concrete.

BENDING RESISTANCE OF THE CROSS SECTION AT ROOM TEMPERATURE

The bending resistance of the cross section depends on the position of the neutral axis, Eq. 1. Fig. 4 depicts the position of this axis, e_{pl}, for both PEB with welded stirrups in C-shape and I-shape.

Fig. 4 - Neutral axis position for PEBA and PEBB.

A_s represents the area of the longitudinal reinforcement under tension and A_s' is the area of the longitudinal reinforcement under compression. h is the height of steel profile, t_w is the web

thickness, b and t_f represent the width and the thickness of the flange. The nominal design strength values for the steel of the profile and reinforcement are defined by f_{yd} and f_{sd}, while f_{cd} represents the design strength of concrete in compression.

$$e_{pl} = \frac{t_w f_{yd} h + (b - t_w) \cdot t_f \cdot 0{,}85 f_{cd} + (A_s - A_s') \cdot f_{sd}}{2 \cdot t_w f_{yd} + (b - t_w) \cdot 0{,}85 f_{cd}} \tag{1}$$

Finally the plastic moment can be calculated accordingly to Eq. 2.

$$M_{pl,Rd} = W_{pl,y} f_{yd} - f_{yd} t_w (h_1/2 - e_{pl})^2 + \cdot 0{,}85 f_{cd}\, 2 b_1 e_{pl} (0.5 h_1 - 0.5 e_{pl}) + 2 A_r (f_{sd} - f_{cd}) \cdot (h/2 - e_r) \tag{2}$$

BENDING RESISTANCE OF THE CROSS SECTION AT ELEVATED TEMPERATURE

The bending resistance of the cross section at elevated temperatures should take into consideration the effect temperature in the material properties. The position of the neutral axis is modified according to Eq. 3 and the bending resistance moment should be updated according to Eq. 4.

$$e_{pl,\theta} = \frac{t_w f_{yd,\theta} h + (b - t_w) \cdot t_f \cdot 0{,}85 f_{cd,\theta} + (A_s - A_s') \cdot f_{sd,\theta}}{2 \cdot t_w f_{yd,\theta} + (b - t_w) \cdot 0{,}85 f_{cd,\theta}} \tag{3}$$

$$M_{fi,\theta,Rd} = W_{pl,y} f_{yd,\theta} - f_{yd,\theta}\, t_w (h_1/2 - e_{pl,\theta})^2 + 0{,}85 \cdot f_{c,\theta}\, 2\, b_1\, e_{pl,\theta} (0.5 h_1 - 0.5\, e_{pl,\theta}) + 2 A_r (f_{sy,\theta} - f_{c,\theta}) \cdot (h/2 - e_r) \tag{4}$$

BENDING RESISTANCE OF PARTIALLY ENCASED BEAM AT ROOM TEMPERATURE

The bending resistance for unrestrained beams shall be determined by Eq. 5. The Lateral Torsional Buckling (LTB) resistance depends on the modified reduction factor, $\chi_{LT,\mathrm{mod}}$. This reduction factor was introduced to include the effect of load type (bending moment diagram). A careful examination of the general procedure of Eurocode 3 part 1.1 (CEN, 2005c) quickly reveals that the influence of the bending moment diagram on the LTB resistance of the beam only appears indirectly through the value of the elastic critical moment and directly in this modified reduction factor.

$$M_{b,Rd} = \chi_{LT,\mathrm{mod}} \times M_{pl,Rd} \tag{5}$$

The plastic moment should be calculated according to Eq. 2. The modified reduction factor is determined by:

$$\chi_{LT,\mathrm{mod}} = \min\left\{1; \frac{1}{\lambda_{LT}{}^2}; \frac{\chi_{LT}}{f}\right\} \tag{6}$$

The non-dimensional slenderness $\bar{\lambda}_{LT}$, the intermediate factor ϕ_{LT}, the reduction factor χ_{LT} and the factor f should be determined according to Eqs. 7-10. The former factor depends on the non-dimensional slenderness and on the correction factor $k_c = 0.86$ used for this bending diagram. The intermediate factor depends on the reference value for the slenderness $\bar{\lambda}_{LT,0} = 0.2$ and on the $\beta = 1.0$ factor. These parameters were determined in accordance to National Annex (IPQ, 2010).

$$\chi_{LT} = \frac{1}{\left(\phi_{LT} + \sqrt{\phi_{LT}^2 - \beta \times \bar{\lambda}_{LT}^2}\right)} \tag{7}$$

$$\phi_{LT} = 0{,}5 + \left(1 + \alpha_{LT} \times \left(\bar{\lambda}_{LT} - \bar{\lambda}_{LT,0}\right) + \beta \times \bar{\lambda}_{LT}^2\right) \tag{8}$$

$$\bar{\lambda}_{LT} = \sqrt{\frac{M_{pl,Rd}}{M_{cr}}} \tag{9}$$

$$f = 1 - 0{,}5 \times (1 - k_c) \times \left(1 - 2 \times \left(\bar{\lambda}_{LT} - 0{,}8\right)^2\right) \tag{10}$$

The imperfection factor α_{LT}, depends on the type of buckling curve adapted. The calculation of the non-dimensional slenderness depends on the ratio between the plastic moment and the critical moment. The critical moment depends on the load type and on the boundary conditions. For the case of 3 point bending simulation Eq. 11 applies.

$$M_{cr} = C_1 \frac{\pi^2 E I_z}{(k_z L_s)^2} \left\{ \sqrt{\left[\left(\frac{k_z}{k_w}\right)^2 \frac{I_w}{I_z} + \frac{(k_z L_s)^2 G I_t}{\pi^2 E I_z} + [C_2 z_g]^2\right]} - C_2 z_g \right\} \tag{11}$$

In Eq.11, Ls represents the length of the beam between supports with lateral restraint, C1 and C2 are factors that depend on loading and end restraint conditions. The parameter Kz =1 is the effective length factor and refers to the out of plane buckling length, ranging from 0.5 (perfect restraint) to 1 (no restraint). The parameter Kw refers to the warping condition of the beam ends and uses the same range. The parameter Zg=Za-Zs=h/2 represents the location of the point load, Za=h/2 and Zs=0 are the coordinate position to the point load and shear centre, both with respect to centroid of the cross section. Table 2 presents the resume of all the factors considered to this testing case.

Table 2 - Effective length factors, load factors and restraints to deformed shapes.

Type of load	Value of the factor				
	k_z	k_w	k_c	C_1	C_2
3-point bending	1,00	1,00	0,86	1,35	0,59

BENDING RESISTANCE OF PARTIALLY ENCASED BEAM AT ELEVATED TEMPERATURE

The uniform temperature in the cross-section has been used so that comparison between the finite element results and the simple calculation formula of Eurocode can be made. In this paper the temperatures used were 200, 400 and 600 ºC, deemed to adequately represent the majority of practical situations under fire conditions. In order to provide the background for the subsequent parametric study, the Eurocode provisions for the lateral-torsional buckling of beams at elevated temperatures are described in detail, based on the assumption of an equivalent steel beam.

The LTB resistance moment under fire, according to P. M. M Vila Real (2004), depends on the modified reduction factor and on the bending resistance of the homogenised cross section for time "t", during fire.

$$M_{b,fi,t,Rd} = \chi_{LT,fi,\mathrm{mod}} \times M_{fi,t,Rd} \tag{12}$$

This bending resistance is calculated for the design value of the resisting moment of the cross section to a uniform temperature, where k_1 and k_2 are adaptive factors to non uniform temperature distributions in section and along the beam. For the case of uniform temperature, both factors are equal to unity.

$$M_{fi,t,Rd} = M_{fi,\theta,Rd} / (k_1 \cdot k_2) \tag{13}$$

The bending resistance of this cross sections should be calculated according to Eq. 4. The modified reduction factor $\chi_{LT,fi,\mathrm{mod}}$ is determined by:

$$\chi_{LT,fi,\mathrm{mod}} = \min\left\{1; \frac{\chi_{LT,fi}}{f}\right\} \tag{14}$$

The non-dimensional slenderness under fire $\overline{\lambda}_{LT,fi}$ and at elevated temperature $\overline{\lambda}_{LT,\theta,com}$, the intermediate factor $\phi_{LT,\theta,com}$, the reduction factor $\chi_{LT,fi}$ and the factor f should be determined according to Eqs. 15-19. The former factor depends on the correction factor $k_c = 0.79$ used for this bending diagram. The imperfection factor α depends on the steel grade.

$$\chi_{LT,fi} = \frac{1}{\left(\phi_{LT,\theta,com} + \sqrt{\phi^2_{LT,\theta,com} - \overline{\lambda}^2_{LT,fi}}\right)} \tag{15}$$

$$\phi_{LT,\theta,com} = 0{,}5 + \left(1 + \alpha \times \overline{\lambda}_{LT,fi} + \overline{\lambda}^2_{LT,fi}\right), \tag{16}$$

$$\alpha = 0{,}65\sqrt{235 / f_y} \tag{17}$$

$$\overline{\lambda}_{LT,fi} = \overline{\lambda}_{LT,\theta,com} = \sqrt{M_{fi,t,Rd} / M_{cr,\theta}} \tag{18}$$

$$f = 1 - 0{,}5 \times \left(1 - k_{c,\theta}\right), \quad k_{c,\theta} = 0{,}79 \tag{19}$$

The critical moment at elevated temperature was calculated accordingly to Eq. 11, affecting the material properties of both materials with the appropriate reduction coefficients.

BENDING RESISTANCE: ADVANCE CALCULATION METHOD

The bending resistance of Partially Encased Beams was defined using the three dimension model and determined by an incremental and iterative solution, based on the arc-length method. The geometric and material nonlinear analysis is considered, establishing the equilibrium in the deformed shape model for each load increment. The maximum load increment was 2000 N and the minimum was 20 N. This last value was defined as small as possible to follow the post buckling behaviour.

For the beams under investigation, all kind of imperfections were included, in particular the out-of-straightness, the residual stresses of the steel beam and the inhomogeneities of the encased concrete. This global imperfection was modelled by means of an equivalent out-of-straightness, defined as L/600 for maximum lateral displacement at mid span. The imperfection mode shape was determined by the result of an elastic stability analysis.

THREE DIMENSION MODEL

The three dimensional model used finite solid elements, with eight nodes and three degrees of freedom in each node (translations). The SOLID 65 finite element was used to model the concrete and the SOLID 185 was used to model each steel component (profile, stirrups and rebars). The dimension of the mesh was defined based on the solution convergence test of the elastic stability analysis. The maximum relative error for this convergence test was smaller than 0.5%. The number of elements used for each simulation is presented in table 1.

Fig 5 represents a small portion of the full 3D model, showing the two different configuration types of stirrups.

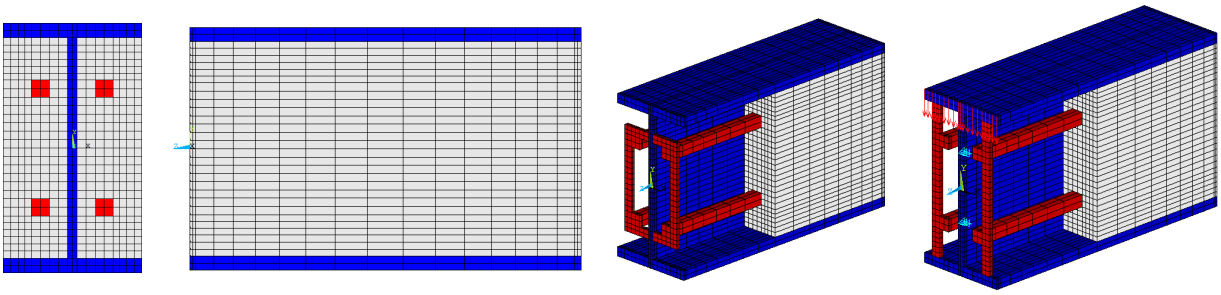

a) Section. b) Lateral view between adjacent stirrups. c) Perspective of PEBA. d) Perspective of PEBB.

Fig. 5 - Three dimension model and mesh for PEBA and PEBB.

SOLID 185 has linear interpolating functions and is able to do plastic and large deflection analysis. SOLID 65 has also linear interpolating functions, being normally used to model reinforced concrete. This element is able to predict cracking and crushing and undergo to plasticity and large deformation. This fracture continuum mechanics model was turned off during simulation, because of the time consuming simulation. Perfect contact was also considered between steel and concrete.

Three types of integration methods were tested: full integration, uniform reduced integration with hourglass control and the enhanced strain integration method. The second method was adapted taking into considerations the problem type and the expected simulation time. All types of integration methods present similar post buckling behaviour with respect to vertical displacement, but different post buckling behaviour in lateral displacement. Typical result for vertical displacement is depicted in Fig. 6. The major important load events were recorded for each simulation.

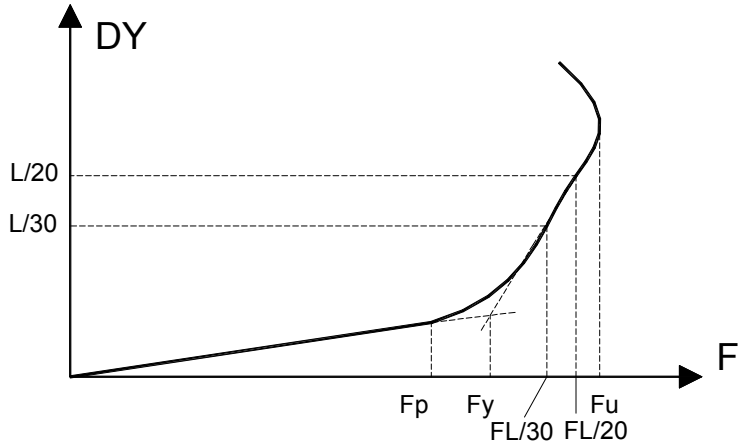

Fig. 6 - Typical vertical displacement for bending simulation of PEB.

MATERIAL BEHAVIOUR

Steel grade S275 was selected for hot rolled steel profile and S500 was selected to model steel reinforcement. C20/25 was the class adapted for concrete. Table 3 represents the main reduction coefficients to be applied to the mechanical properties of S275. This table also presents the main points used to define the stress- strain behaviour of the material.

Table 3- Mechanical properties of S275 at room and elevated temperature.

$k_{y,\theta}$	$k_{E,\theta}$	θ $[^{o}C]$	f_y $[N/mm^2]$	f_u $[N/mm^2]$	E $[kN/mm^2]$	G $[kN/mm^2]$	ν	ε_y	ε_u
1,00	1,00	20	275	430	210	80,76		0,0013095	0,15
1,00	0,90	200	275	430	189	94,50		0,001455	0,15
1,00	0,70	400	275	430	147	73,50	0,3	0,0018707	0,15
0,47	0,31	600	129,25	202,1	65,1	32,55		0,0019854	0,15

Fig. 7 depicts the model for stress with strain hardening behaviour. The elastic modulus starts to decrease after 100 ºC, being the stress strain curves not coincident for 20, 200 and 400 ºC.

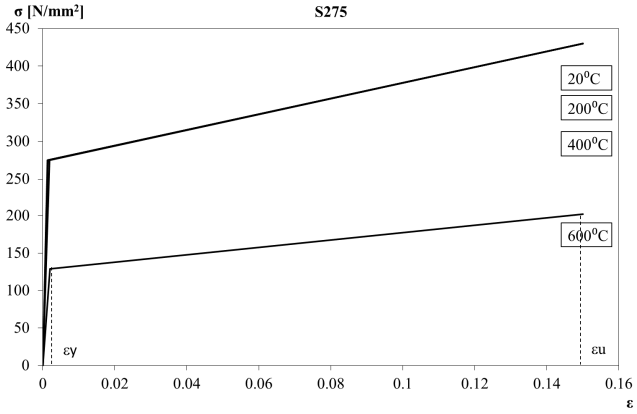

Fig. 7 - Stress strain model to steel S275.

Table 4 represents the main reduction coefficients to be applied to the mechanical properties of C20/25 concrete. This table also presents the main points used to define the stress- strain behaviour of the material.

Table 4 - Mechanical properties of C20/25 at room and elevated temperature.

$f_{c,\theta}/f_{ck}$	$k_{ct,\theta}$	$\theta\ [^oC]$	$f_{cm}\ [N/mm^2]$	$f_{ctm}\ [N/mm^2]$	E	ν	$\varepsilon_{c1,\theta}$	$\varepsilon_{cu1,\theta}$
1,00	1,00	20	28	28	30	0,2	0,000933	0,020
0,95	0,80	200	26,6	26,6	28,5		0,005500	0,025
0,75	0,40	400	21	21	22,5		0,010000	0,030
0,45	0,00	600	12,6	12,6	13,5		0,025000	0,035

Fig. 8 depicts the model for stress - strain behaviour under tension and compression. This model was considered elastic perfectly plastic, due to the confinement of concrete.

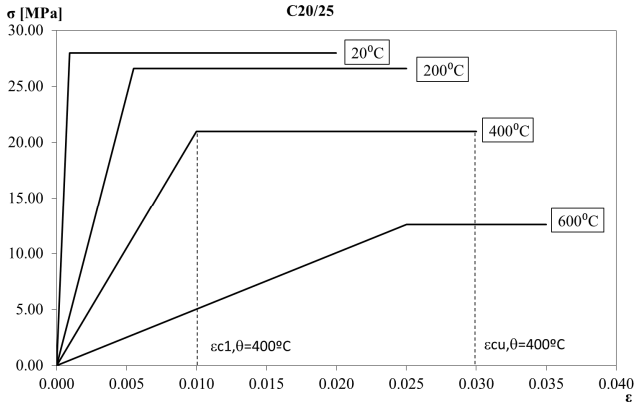

Fig. 8 - Stress strain model to concrete C20/25.

Table 5 represents the main reduction coefficients to be applied to the mechanical properties of reinforcing steel. This table also presents the main points used to define the stress- strain behaviour of the material, under tension and compression.

Table 5 - Mechanical properties of S500 at room and elevated temperature.

$\frac{f_{sy,\theta}}{f_{yk}}$	$\frac{E_{s,\theta}}{E_s}$	$\theta\ [^oC]$	$f_y\ [N/mm^2]$	$f_u\ [N/mm^2]$	$E\ [kN/mm^2]$	$G\ [kN/mm^2]$	ν	ε_y	ε_u
1,00	1,00	20	500	500	210,0	80,76923	0,3	0,0023810	0,15
1,00	0,87	200	500	500	182,7	91,35		0,0027367	0,15
0,94	0,56	400	470	470	117,6	58,8		0,0039966	0,15
0,40	0,24	600	200	200	50,40	25,2		0,0039683	0,15

Fig. 9 depicts the model for stress - strain behaviour of the reinforced steel, under tension and compression. The material model was considered elastic perfectly plastic.

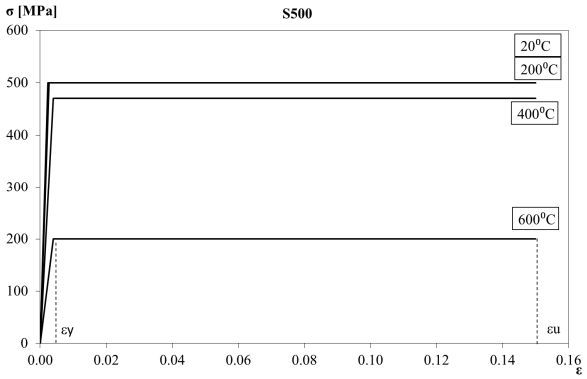

Fig. 9 - Stress strain model to steel S500.

NUMERICAL RESULTS AT ROOM TEMPERATURE

Fig. 10 depicts the results of the bending resistance defined by the lower limit of the simple calculation formula of Eurocode (CEN, 2005c) and the upper limit of the critical moment resistance. All the simulated results were determined by the load event that corresponds to Fy. Fig. 10a) corresponds to the bending resistance of PEBA with "C" shape stirrups welded to the web and Fig. 10b) corresponds to the bending resistance of PEBB with "I" shape stirrups welded to the flanges.

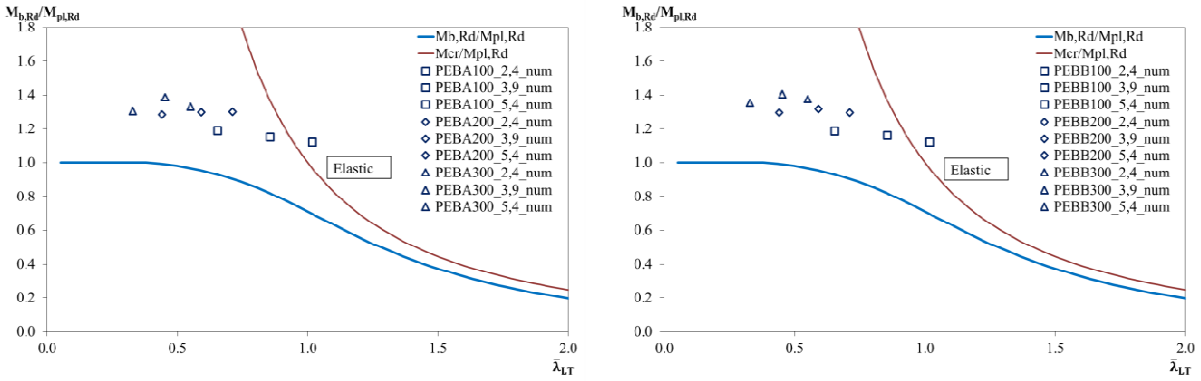

a) PEBA b) PEBB

Fig. 10- Lateral Torsional Buckling resistance of PEBA and PEBB at room temperature, criterion Fy

There is no significant difference in the bending resistance between PEBA and PEBB. This conclusion is only valid for the tested cross sections. Table 6 represents all the other load events determined at room temperature.

Table 6 - Bending resistance for PEBA and PEBB at room temperature.

Id.	$L_s[m]$	$\theta[°C]$	$F_p[kN]$	$F_y[kN]$	$F_{L/30}[kN]$	$F_{L/20}[kN]$	$F_u[kN]$
PEBA100_2,4F	2,4	20	22,00	27,05	27,88	28,69	34,47
PEBA100_3,9F	3,9	20	13,70	16,13	16,68	17,13	18,31
PEBA100_5,4F	5,4	20	8,50	11,35	11,68	11,99	12,27
PEBA200_2,4F	2,4	20	145,00	154,90	166,42	170,44	172,38
PEBA200_3,9F	3,9	20	83,00	96,30	100,90	103,98	115,22
PEBA200_5,4F	5,4	20	59,00	69,60	71,60	73,65	87,82
PEBA300_2,4F	2,4	20	390,00	433,50	462,53	457,65	463,25
PEBA300_3,9F	3,9	20	250,00	283,50	309,74	307,29	310,76
PEBA300_5,4F	5,4	20	183,00	196,50	230,86	229,72	230,97
PEBB100_2,4F	2,4	20	23,00	27,00	27,88	28,70	34,57
PEBB100_3,9F	3,9	20	13,50	16,25	16,68	17,13	18,28
PEBB100_5,4F	5,4	20	9,20	11,35	11,68	11,99	12,27
PEBB200_2,4F	2,4	20	145,00	156,00	167,67	172,23	176,29
PEBB200_3,9F	3,9	20	76,00	97,60	101,28	104,41	117,89
PEBB200_5,4F	5,4	20	56,00	69,40	71,82	73,89	89,08
PEBB300_2,4F	2,4	20	385,00	449,00	461,78	456,26	462,89
PEBB300_3,9F	3,9	20	248,00	287,00	310,26	307,54	312,04
PEBB300_5,4F	5,4	20	178,00	203,20	234,23	232,09	234,39

NUMERICAL RESULTS AT ELEVATED TEMPERATURE

Fig. 11 depicts the results of the bending resistance defined by the lower limit of the simple calculation formula proposed by Paulo Vila Real et al. (P. M. M Vila Real et al., 2004) and the upper limit defined by the elastic critical moment resistance. All the simulated results were determined for the load event that corresponds to Fy. Fig. 11a) corresponds to the bending resistance of PEBA with "C" shape stirrups welded to the web and Fig. 11b) corresponds to the bending resistance of PEBB with "I" shape stirrups welded to the flanges.

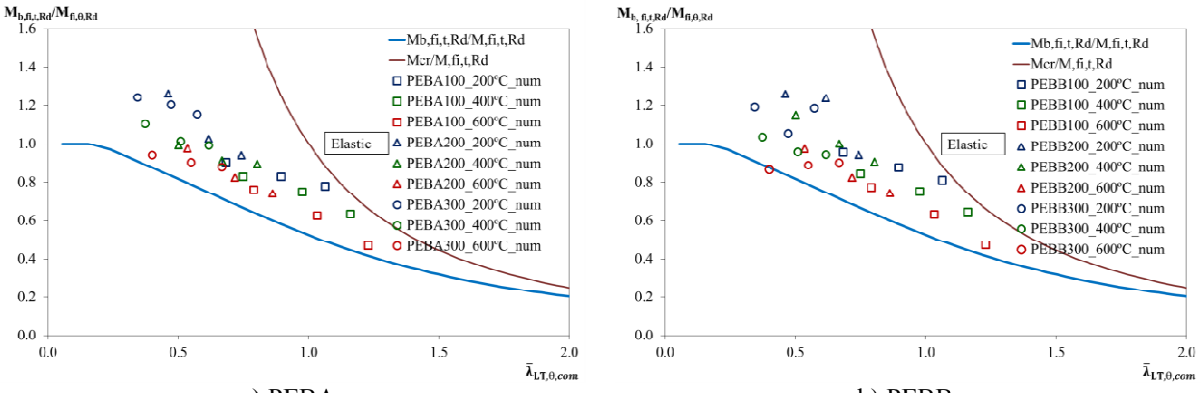

a) PEBA b) PEBB

Fig. 11- Lateral Torsional Buckling resistance of PEBA and PEBB at elevated temperature, criterion Fy

There is no significant difference in the bending resistance at elevated temperatures between PEBA and PEBB. This conclusion is only valid for the tested cross sections. Table 7 represents all the other load events determined at different temperature levels.

Table 7- Bending resistance for PEBA and PEBB at elevated temperatures.

Id.	$L[m]$	F_p $[kN]$	F_y $[kN]$	$F_{L/30}$ $[kN]$	$F_{L/20}$ $[kN]$	F_u $[kN]$	F_p $[kN]$	F_y $[kN]$	$F_{L/30}$ $[kN]$	$F_{L/20}$ $[kN]$	F_u $[kN]$	F_p $[kN]$	F_y $[kN]$	$F_{L/30}$ $[kN]$	$F_{L/20}$ $[kN]$	F_u $[kN]$
		200ºC	200ºC	200ºC	200ºC	200ºC	400ºC	400ºC	400ºC	400ºC	400ºC	600ºC	600ºC	600ºC	600ºC	600ºC
PEBA100_2,4F	2,4	18,00	20,50	25,38	24,02	25,85	18,40	18,55	20,02	18,85	20,92	7,50	7,90	7,60	7,35	8,17
PEBA100_3,9F	3,9	11,20	11,58	13,91	13,10	14,30	10,30	10,30	10,35	9,96	10,60	4,02	4,02	3,77	3,66	4,02
PEBA100_5,4F	5,4	7,65	7,87	8,92	8,50	9,03	6,30	6,30	6,24	6,15	6,49	2,18	2,18	2,24	2,22	2,31
PEBA200_2,4F	2,4	130,00	151,60	161,85	-	164,20	112,50	117,50	135,72	125,16	140,06	50,50	54,30	54,71	52,46	55,71
PEBA200_3,9F	3,9	71,00	76,00	94,42	90,68	94,78	64,50	66,30	73,73	69,41	76,65	28,20	28,20	27,46	26,67	29,06
PEBA200_5,4F	5,4	48,80	50,20	63,76	60,34	64,91	44,70	47,20	47,53	45,34	48,84	18,33	18,33	17,07	16,57	18,33
PEBA300_2,4F	2,4	325,00	412,00	449,26	443,73	450,56	260,00	361,00	399,26	-	407,04	115,00	145,50	169,95	-	183,41
PEBA300_3,9F	3,9	205,00	245,40	300,21	293,75	301,07	180,00	204,00	232,30	207,71	257,02	80,00	85,80	94,89	88,53	102,30
PEBA300_5,4F	5,4	147,00	170,00	214,19	193,41	220,27	127,00	144,00	158,37	143,08	176,00	60,30	60,30	61,68	58,78	67,71
PEBB100_2,4F	2,4	19,50	21,70	25,41	24,10	25,88	18,75	18,85	20,09	18,95	20,97	8,06	8,06	7,65	7,40	8,22
PEBB100_3,9F	3,9	11,50	12,25	13,94	13,14	14,33	10,33	10,33	10,40	10,00	10,64	4,06	4,06	3,81	3,68	4,06
PEBB100_5,4F	5,4	7,60	8,16	8,94	8,52	9,04	6,40	6,40	6,27	6,17	6,52	2,20	2,20	2,26	2,24	2,34
PEBB200_2,4F	2,4	120,00	151,20	163,06	165,33	165,50	113,50	136,20	136,78	124,35	141,09	52,50	54,23	54,61	51,69	55,91
PEBB200_3,9F	3,9	71,00	91,60	94,84	91,18	95,15	65,00	72,90	74,10	69,87	76,92	28,20	28,20	27,61	26,82	29,25
PEBB200_5,4F	5,4	46,50	50,30	64,03	60,65	65,09	44,50	47,70	47,72	45,58	49,02	18,41	18,41	-	-	18,41
PEBB300_2,4F	2,4	320,00	395,00	447,44	-	448,78	260,00	338,50	-	-	404,65	110,00	134,00	-	-	182,98
PEBB300_3,9F	3,9	174,00	215,00	300,08	293,44	301,76	174,00	192,50	232,00	208,02	257,92	82,50	84,50	95,19	88,79	102,67
PEBB300_5,4F	5,4	137,50	174,70	215,73	194,06	223,78	125,00	137,20	159,38	143,81	177,82	59,00	61,90	62,76	59,48	67,81

CONCLUSION

This numerical study confirms that the bending resistance of Partially Encased Beams is defined by the lateral torsional buckling (LTB) resistance. The LTB resistance at room temperature may be determined by the formula of Eurocode 3 part 1.1 (CEN, 2005c) and at elevated temperature by the new proposed formula of Paulo Vila Real et al. (P. M. M Vila Real et al., 2004), using the necessary adaptations to the characteristics of the composite section.

The parametric study of 72 full 3D simulations revealed that bending resistance decreases with the temperature of the element, being the simple calculation formula always in the safe side. From the observation of the previous Fig. 10 and Fig.11, there is a small difference between the values obtained by the simple calculation formulas and numerical results. The difference may be explained by the inexistence of damage model for tension and compression of concrete, the inexistence of relative displacement between steel and concrete and by the additional resistance of concrete in tension with respect to compression.

REFERENCES

[1]-Akio Kodaira, H. F., Hirokazu Ohashi and Toshihiko Nishimura (2004). "Fire Resistance of Composite Beams Composed of Rolled Steel Profile Concreted Between Flanges." Fire Science and Technology 23(3): 192-208.

[2]-Assi I.M., A. S. M., Hunaiti Y.M. (2002). "Flexural strength of composite beams partially encased in lightweight concrete." Pakistan Journal of Applied Sciences 2(3): 320-323.

[3]-CEN (2005a). EN 1994-1-2 - Eurocode 4: Design of Composite Steel and Concrete Structures - Part 1–2: General Rules—Structural Fire Design. Brussels: 225.

[4]-CEN (2004). EN 1992-1-2 - Eurocode 2: Design of concrete structures - Part 1-2: General rules - Structural fire design. Brussels, CEN: 97.

[5]-CEN (2005b). EN 1993-1-2 - Eurocode 3: Design of steel structures - Part 1-2: General rules - Structural fire design. Brussels, CEN: 72.

[6]-CEN (2005c). EN 1993-1-1 - Eurocode 3: Design of steel structures - Part 1-1: General rules and rules for buildings. Brussels: 91.

[7]-Correia, A. J. P. M. and J. P. C. Rodrigues (2011). "Fire resistance of partially encased steel columns with restrained thermal elongation." Journal of Constructional Steel Research 67(4): 593-601.

[8]-De Nardin, S. and A. L. H. C. El Debs (2009). "Study of partially encased composite beams with innovative position of stud bolts." Journal of Constructional Steel Research 65(2): 342-350.

[9]-Elghazouli, A. Y. and J. Treadway (2008). "Inelastic behaviour of composite members under combined bending and axial loading." Journal of Constructional Steel Research 64(9): 1008-1019.

[10]-Hosser, D., T. Dorn and O. Elnesr (1994). "Experimental and Numerical-Studies of Composite Beams Exposed to Fire." Journal of Structural Engineering-Asce 120(10): 2871-2892.

[11]-IPQ (2010). NP EN 1993-1-1 - Eurocódigo 3 - Projecto de estruturas em aço Parte 1.1: Regras gerais e regras para edifícios. Portugal: 116.

[12]-Kindmann, R., R. Bergmann, L. G. Cajot and J. B. Schleich (1993). "Effect of Reinforced-Concrete between the Flanges of the Steel Profile of Partially Encased Composite Beams." Journal of Constructional Steel Research 27(1-3): 107-122.

[13]-Kordina, K. (1989). Behaviour of Composite Columns and Girders in Fire. Fire Safety Science-Proceedings of the Second International Symposium, Tokyo, Japan, International Association for Fire Safety Science.

[14]-Kvočák, V. and L. Drab (2012). "Partially-encased composite thin-walled steel beams." Steel Structures and Bridges 2012 - 23rd Czech and Slovak International Conference 40: 91-95.

[15]-Lindner Joachim, B. N. (2000). Lateral torsional Bucking of partially encased composite beams without concrete slab. Comp. const. in steel and concrete IV, Banff, Alberta, Canada.

[16]-Nakamura, S. and N. Narita (2003). "Bending and shear strengths of partially encased composite I-girders." Journal of Constructional Steel Research 59 (12): 1435-1453.

[17]-Paulo A. G. Piloto (2013a), Ana B.R. Gavilán, Marco Zipponi, Alberto Marini, Luís M.R. Mesquita, Giovanni Plizzari, "Experimental investigation of the fire resistance of partially encased beams", Journal of Constructional Steel Research, Volume 80, January 2013, ISSN 0143-974X, 10.1016/j.jcsr.2012.09.013. pp: 121-137.

[18]-Paulo A. G. Piloto (2013b), Ana B. R. Gavilán, Luís M. R. Mesquita, Carlos Gonçalves, Luisa Barreira, "Experimental Investigation on the Performance of Partially Encased Beams at Elevated and Room Temperature", artigo em atas do 2º congresso Ibero-Latino-Americano em Segurança Contra Incêndios, ISBN 978-972-96524-9-3, pp: 187-196, 29 de maio a 1 de junho de 2013, Universidade de Coimbra, Portugal.

[19]-P. M. M Vila Real (2004), N Lopes, L Simões da Silva, J.-M Franssen, Lateral-torsional buckling of unrestrained steel beams under fire conditions: improvement of EC3 proposal, Computers & Structures, Volume 82, Issues 20–21, August 2004, Pages 1737-1744, ISSN 0045-7949.

[20]-R. Maquoi, C. H., V. de Ville de Goyet, M. Braham, C. Richard, C. Müller, K. Weynand, Y. Galéa, A. Bureau, F. Espiga, P. Croce, S. Caramelli, L.-G. Cajot, M. Haller (2002). Lateral torsional buckling in steel and composite beams. Technical Steel Research Final Report EUR 20888 EN. E. Commission.

[21]-Schleich, J. B. (1987). Computer assisted analysis of the fire resistance of steel and composite concrete-steel structures (REFAO-CAFIR). Luxembourg, Commission of the European Communities. Final report EUR 10828 EN.